Proceedings of 5th World Congress of Chemical Engineering, San Diego, CA, July 1996.

# Vertical Side Wall Convection in Deep Beds of Granular Material Subjected to Vertical, Sinusoidal Oscillations

C.R. Wassgren, M.L. Hunt, and C.E. Brennen
California Institute of Technology, Mail Code: 104-44, Pasadena, CA 91125

## ABSTRACT

When a deep bed of granular material is subjected to vertical, sinusoidal oscillations, a number of interesting phenomena appear including heaps, convection cells, surface waves, and arches. This paper examines the convection cell phenomena associated with vertical side walls using two-dimensional discrete element simulations. Measurements from the simulations indicate that when the container aspect ratio, defined as the depth of the granular bed, $H$, divided by the width of the container, $W$, is large, convection cells interact and the boundary layer width of the downward flow of particles against the walls varies linearly with the container width. However, when the container aspect ratio small and the convection cells do not interact, the boundary layer width remains at a nearly constant value of ten particle diameters. Other simulation measurements show that the vertical location of the convection cell center remains close to the free surface regardless of container aspect ratio. Additional measurements show that the particle flow rate per oscillation cycle in the boundary layer increases with increasing vibration amplitude and velocity. Lastly, the asymmetric drag mechanism proposed as the cause of the side wall convection cells is briefly examined.

## INTRODUCTION

The application of forced vibrations on granular materials is found in a number of industrial applications. Examples include vibrating sorting tables, packing tables, conveyors, and "live-wall" hoppers to name just a few devices. Although the use of such devices is common, there remains a poor understanding of how vibration affects a bed of granular material. Recently, however, there have been a number of experimental and computational studies of the fundamental behavior of vibrated granular beds. These studies typically consist of a container partially filled with a cohesionless granular material (e.g. glass spheres) mounted on a shaker that subjects the assembly to vertical, sinusoidal oscillations.

Two distinct regimes are observed in the vibrating bed experiment depending on the depth of the particle bed. When the dimensionless bed depth of material in the container, $H/d$, where $H$ is the initial, level depth of the particle bed and $d$ is the mean particle diameter, is less than six, the granular material exhibits vibro-fluidized behavior (see, for example, Brennen *et al.*[1]). However, when $H/d \geq 6$, a much different behavior is observed. Here particles move coherently and the bed of material moves as a single unit. In this deep bed regime a number of interesting phenomena are observed such as heaps [2-4], convection cells [5-9], surface waves [7,10,11], and kinks or arches [7,10,12]. The appearance of these phenomena is governed primarily by the dimensionless acceleration amplitude of the forcing vibrations, $\Gamma = a(2\pi f)^2/g$, where $a$ is the oscillation amplitude, $f$ is the frequency (in Hertz), and $g$ is the acceleration due to gravity, and to a lesser extent, the dimensionless bed depth, $H/d$ (see, for example, Wassgren *et al.* [10] and Melo *et al.* [11]).

This paper examines, in detail, the convection cell phenomena associated with vertical container side walls using discrete element simulations. In addition to making observations and measurements, the mechanism causing this behavior is examined using the simulations.

## SIMULATIONS

The discrete element simulations described in this paper are all two-dimensional. Each particle has two translational and one rotational degrees of freedom. All of the particles have circular cross-section with a diameter chosen randomly between a specified minimum and maximum (giving a uniform distribution of diameters). The mass and moment of inertia of the particles is based on that of a solid sphere. The forces acting on the particles include a gravity body force and forces due to particle/particle and particle/boundary contacts. The contact model in the normal direction is a damped, linear spring and in the tangential direction it is a linear spring in series with a frictional sliding element. The parameters used in the baseline simulation are given in table 1.

The simulated vibrating container consists of a horizontal base and two vertical walls. These boundaries are rigid and flat but have frictional properties. All of the boundaries oscillate vertically and in-phase with a sinusoidal trajectory given by, $y=a\sin(2\pi ft)$, where $a$ is the oscillation amplitude, $f$ is the oscillation frequency (in Hertz), and $t$ is time. This reproduces the motion of the container in many experiments.

In both the experiments and simulations when $\Gamma$ is just greater than one convection cells appear where particles move down in a narrow boundary layer along the vertical walls of the container and up to the free surface in the interior of the bed. Using the simulations, the effects of container geometry, vibration parameters, and particle properties on the size and particle flow rate in the convection boundary layer were studied. The geometry of the container is given by the width of the container, $W$, and the depth of the granular bed, $H$. The vibration parameters include the amplitude, $a$, and frequency, $f$, of the oscillations.

## RESULTS

The effects of changing the parameters listed in the previous paragraph on the boundary layer are quantified using three different measures. These include the width, $w$, and height, $h$, of the boundary layer and the average number of particles moving down in the boundary layer each cycle, $J$. The width and height of the boundary layer are determined from the location of the convection cell center as shown in the top illustration of figure 1. The convection cell center is found using particle displacement/cycle vectors which are the particle displacements over one oscillation cycle at various locations in the container averaged over many oscillations. The number of particles flowing down along the wall over one oscillation cycle, $J$, is measured across width, $w$, at height, $h$.

The width and height of the convection cell center were measured for various container aspect ratios. When the container aspect ratio, $\alpha=H/W$, is greater than 0.2, the two convection cells in the container interact with each other as shown at the top of figure 1. In this regime, the width of the convection cell, $w$, increases linearly with the container width, $W$ (shown as the solid triangles at the left of figure 2), a result which is in agreement with the experimental measurements found by Knight *et al.* [6] When

$\alpha \leq 0.2$, however, the convection cells do not interact (the bottom of figure 1) and the boundary layer thickness remains nearly constant with a value of roughly ten particle diameters (the open circles in the left plot of figure 2). In addition, the width of the boundary layer does not vary with the vibration parameters. These results indicate that the boundary layer width is governed by the container geometry when the convection cells can interact with each other; however, when the convection cells do not interact, there is an intrinsic boundary layer width of approximately ten particle diameters.

The vertical location of the convection cell center, $h$, remains close to the free surface of the granular bed. This is clearly seen in figure 1. As shown in the right plot of figure 2, the height of the convection cell center increases linearly with bed depth, $H$. The slope of the line indicates that the convection cell center remains approximately $0.14H$ from the free surface regardless of container aspect ratio. Simulations using different vibration parameters show that $h/H$ decreases with increasing vibration amplitude and vibration velocity.

The average number of particles moving down in the boundary layer each cycle, $J$, was measured for various vibration parameters. The acceleration amplitude of the oscillations, $\Gamma = a\,(2\pi f)^2/g$, where $g$ is the acceleration due to gravity, ranged from zero to 2.0. When $\Gamma > 2.0$ other phenomena, such as standing surface waves, appear (see, for example, Wassgren *et al.* [7,10]) and so the range of $\Gamma$ was restricted in order to avoid including the effects of other phenomena. The vibration frequency, $f$, varied from 3 to 30 Hz. In this range of amplitudes and frequencies, $J$ is found to increase with increasing vibration amplitude and velocity (refer to figure 3 for a plot showing $J$ as a function of vibration amplitude).

A preliminary study of the effects of particle/particle and particle/wall properties was also performed. The boundary layer width and height do not vary significantly with variations in particle/particle and particle/wall friction ($\mu_{pp}$ and $\mu_{pw}$ respectively). However, the particle flow rate in the convection boundary layer, $J$, decreases as the particle wall friction, $\mu_{pw}$, decreases, eventually reaching zero (no convective motion) when $\mu_{pw}=0$. The boundary layer width is affected by the particle/particle and particle/wall coefficients of restitution ($\varepsilon_{pp}$ and $\varepsilon_{pw}$, respectively). As $\varepsilon_{pp}$ and $\varepsilon_{pw}$ are increased, $w$ also increases. For example, for a container with $W/d=H/d=50$, the boundary layer width is $w/d=7$ when $\varepsilon_{pp}=\varepsilon_{pw}=0.8$. When $\varepsilon_{pp}=\varepsilon_{pw}=0.98$ for the same container, $w/d$ is nearly ten.

A number of hypotheses have been suggested to explain the appearance of the side wall convection cells. Among them is the asymmetric drag argument first proposed by Gallas *et al.* [8]. The argument is as follows: when the bed of material first leaves the base of the container it is still densely packed and collisions between particles and the container walls occur frequently. Since the motion of the container walls is down relative to the particles, the particles that collide with the wall are retarded in their upward movement. Similarly, as the particle bed falls back toward the base, particle/wall collisions occur and particles near the wall do not fall toward the base as rapidly as those particles in the center of the bed. Fewer collisions occur with the walls, however, as the bed falls back toward the container base since the bed has dilated in the vertical direction and has pulled in from the walls of the container (due to shearing with the walls). As a result, there is a net downward shear force acting on the particle bed near the walls and a convection boundary layer of particles forms. A more complete description of this proposed mechanism will be given in a future paper by the authors.

Measurements from the simulations of the total shear force acting on the particle bed due to the vertical walls support this argument. As seen in figure 4 the downward drag acting on the particle bed due to the walls is much greater than the upward drag resulting in a net downward drag force acting on the particle bed. Additional measurements of the number of particle/wall collisions as a function of phase angle indicate that more collisions occur as the particle bed moves up relative to the base than when moving down, further supporting the proposed mechanism.

In addition to being able to describe the downward convective motion for vertical walls, this same argument is able to account for the upward motion of particles observed to occur for inclined walls [6,13]. When the particle bed first leaves the container, it remains closely packed and no collisions occur with the container boundaries since they angle away from the granular bed. However, as the bed falls back toward the base, it has dilated. As a result, the granular bed collides with the walls of the container before colliding with the base. Particles at the walls are then held back as the rest of the bed falls to the container base. The result is a net upward acting drag force acting on particles at the inclined walls and a convection cell with particles moving up along the walls.

## ACKNOWLEDGMENTS

The authors wish to acknowledge the support of the National Science Foundation who supported this work under NSF grant CTS 9300665.

## LITERATURE CITED

1. Brennen, C.E., S. Ghosh, and C.R. Wassgren, to appear in *J. Appl. Mech.* (1996).
2. Evesque, P. and J. Rajchenbach, *Phys. Rev. Lett.*, **62**, 1, 44-46 (1989).
3. Laroche, C., S. Douady, and S. Fauve, *J. Phys. France*, **50**, 7, 699-706 (1989).
4. Pak, H.K., E. Van Doorn, and R.P. Behringer, *Phys. Rev. Lett.*, **74**, 23, 4643-4646 (1995).
5. Knight, J.B., H.M. Jaeger, and S.R. Nagel, *Phys. Rev. Lett.*, **70**, 24, 3728-3731 (1993).
6. Knight, J.B., E.E. Ehrichs, V.Y. Kuperman, J.K. Flint, H.M. Jaeger, and S.R. Nagel, submitted to *Phys. Rev. E.*
7. Wassgren, C.R., C.E. Brennen, and M.L. Hunt, submitted to *Phys. Rev. Lett.*, (1996).
8. Gallas, J. A. C., H. J. Herrmann, and S. Sokolowski, *Phys. Rev. Lett.*, **69**, 9, 1371-1374 (1992).
9. Taguchi, Y-h., *Phys. Rev. Lett.*, **69**, 9, 1367-1370 (1992).
10. Wassgren, C.R., C.E. Brennen, and M.L. Hunt, to appear in *J. Appl. Mech.*, (1996).
11. Melo, F., P. Umbanhowar, and H.L. Swinney, *Phys. Rev. Lett.*, **75**, 21, 3838-3841 (1995).
12. Douady, S., S. Fauve, and C. Laroche, *Europhys. Lett.*, **8**, 7, 621-627 (1989).
13. Wassgren, C.R., C.E. Brennen, and M.L. Hunt, *ASCE Engineering Mechanics Proceedings*, Denver, CO (1995).

## TABLES

Table 1. The parameters used in the baseline simulation discussed in this paper.

| | | |
|---|---|---|
| oscillation frequency | $f$ | 20 Hz |
| number of particles | $N$ | 1000 |
| particle/particle coefficient of restitution | $\varepsilon_{pp}$ | 0.80 |
| particle/particle normal spring constant | $k_{pn}$ | $5.289*10^{3}$ N/m |
| particle/particle normal dashpot coefficient | $\upsilon_{pn}$ | $8.337*10^{-3}$ N/(m/s) |
| particle/particle tangential spring constant | $k_{ps}$ | $5.289*10^{3}$ N/m |
| particle/particle sliding friction coefficient | $\mu_{pp}$ | 1.0 |
| particle/wall coefficient of restitution | $\varepsilon_{pw}$ | 0.80 |
| particle/wall normal spring constant | $k_{wn}$ | $1.058*10^{4}$ N/m |
| particle/wall normal dashpot coefficient | $\upsilon_{wn}$ | $1.667*10^{-2}$ N/(m/s) |
| particle/wall tangential spring constant | $k_{ws}$ | $1.058*10^{4}$ N/m |
| particle/wall sliding friction coefficient | $\mu_{pw}$ | 1.0 |
| simulation time step | $\Delta t$ | $3.504*10^{-6}$ sec |
| container width/mean particle diameter | $W/d$ | 50 |
| dimensionless bed depth | $H/d$ | 20 |
| particle diameters | $d$ | 0.9-1.1 mm |
| particle density | $\rho$ | 2500 kg/m$^3$ |

## FIGURES

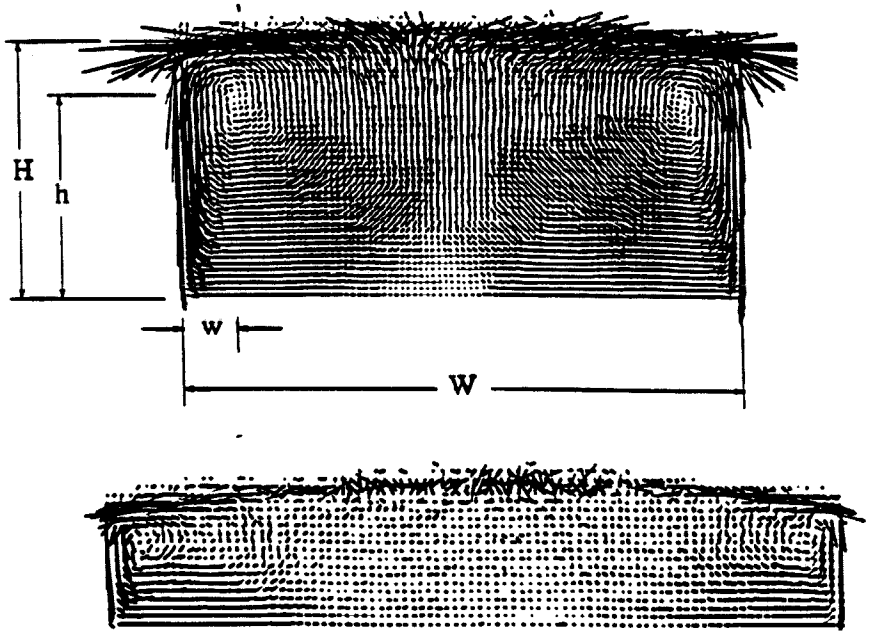


Figure 1. The particle displacement/cycle vectors for two different container aspect ratios, $\alpha=H/W$, using the vibration parameters and particle properties given in table 1. The figure on the top is for a container with $\alpha=^{50d}/_{100d}=0.5$ and on the bottom $\alpha=^{20d}/_{100d}=0.2$. The vectors have been scaled and may appear to extend beyond the container walls. The top figure also includes the definitions for container width, $W$, and granular bed depth, $H$, as well as the boundary layer width, $w$, and height, $h$.

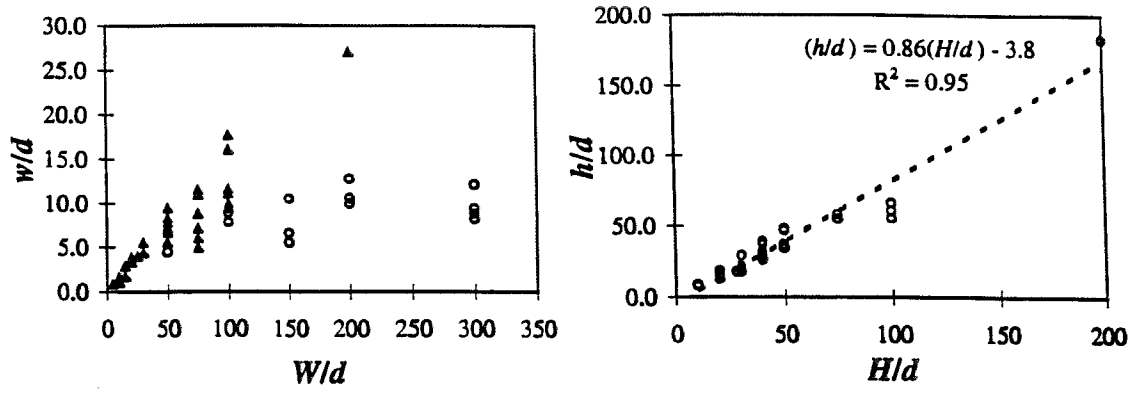


Figure 2. Left: Plot of the boundary layer width, $w$, plotted against the width of the container, $W$. Right: Plot of the convection cell center height from the container base, $h$, plotted against the overall depth of the granular bed, $H$. Both quantities are non-dimensionalized by the mean particle diameter, $d$.

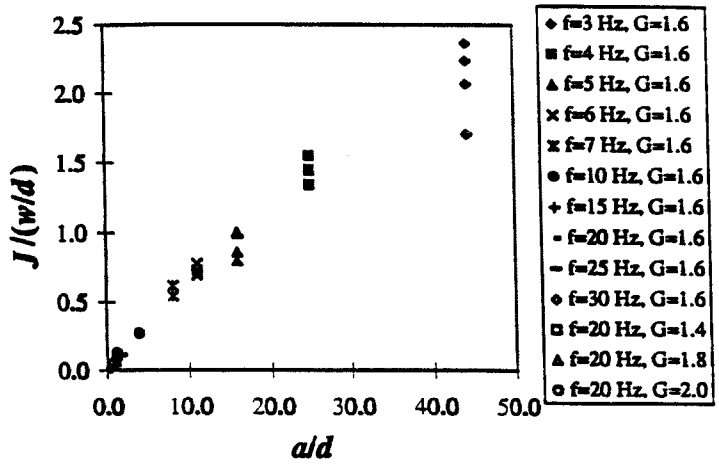


Figure 3. Plot of the average number of particles moving down in a boundary layer each cycle divided by the dimensionless boundary layer width, $J/(w/d)$ [particles/cycle], plotted against the vibration amplitude non-dimensionalized by mean particle diameter.

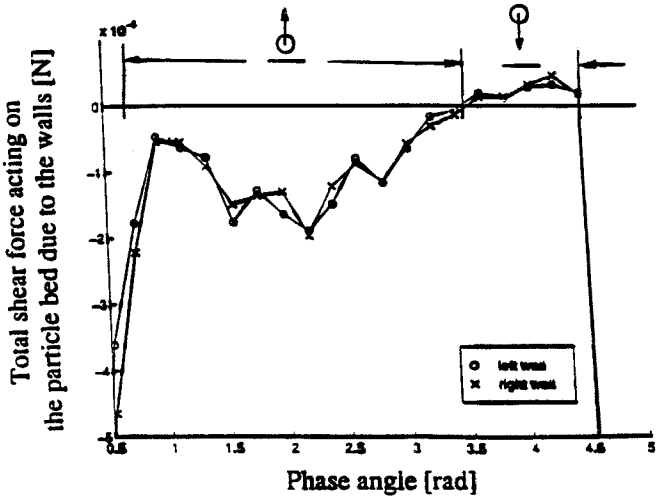


Figure 4. Plot of the total tangential force acting on the particle bed due to the vertical walls as a function of oscillation phase angle. The motion of the bed relative to the container is indicated by the cartoons along the x-axis.